JLB

Article

Host lung immunity is severely compromised during tropical pulmonary eosinophilia: role of lung eosinophils and macrophages

Pankaj Sharma, Aditi Sharma,*,† Achchhe Lal Vishwakarma,‡ Promod Kumar Agnihotri,§ Sharad Sharma,†,§ and Mrigank Srivastava*,†,1*

*Parasitology Division, ‡Sophisticated Analytical Instrument Facility, and §Toxicology Division, Council of Scientific and Industrial Research–Central Drug Research Institute, Lucknow, India; and †Academy of Scientific and Innovative Research, New Delhi, India

RECEIVED JULY 20, 2015; REVISED SEPTEMBER 29, 2015; ACCEPTED OCTOBER 1, 2015. DOI: 10.1189/jlb.4A0715-309RR

ABSTRACT

Eosinophils play a central role in the pathogenesis of tropical pulmonary eosinophilia, a rare, but fatal, manifestation of filariasis. However, no exhaustive study has been done to identify the genes and proteins of eosinophils involved in the pathogenesis of tropical pulmonary eosinophilia. In the present study, we established a mouse model of tropical pulmonary eosinophilia that mimicked filarial manifestations of human tropical pulmonary eosinophilia pathogenesis and used flow cytometry-assisted cell sorting and real-time RT-PCR to study the gene expression profile of flow-sorted, lung eosinophils and lung macrophages during tropical pulmonary eosinophilia pathogenesis. Our results show that tropical pulmonary eosinophilia mice exhibited increased levels of IL-4, IL-5, CCL5, and CCL11 in the bronchoalveolar lavage fluid and lung parenchyma along with elevated titers of IgE and IgG subtypes in the serum. Alveolar macrophages from tropical pulmonary eosinophilia mice displayed decreased phagocytosis, attenuated nitric oxide production, and reduced T-cell proliferation capacity, and FACS-sorted lung eosinophils from tropical pulmonary eosinophilia mice upregulated transcript levels of ficolin A and anti-apoptotic gene *Bcl2,* but proapoptotic genes *Bim* and *Bax* were downregulated. Similarly, flow-sorted lung macrophages upregulated transcript levels of TLR-2, TLR-6, arginase-1, Ym-1, and FIZZ-1 but downregulated nitric oxide synthase-2 levels, signifying their alternative activation. Taken together, we show that the pathogenesis of tropical pulmonary eosinophilia is marked by functional impairment of alveolar macrophages, alternative activation of lung macrophages, and upregulation of anti-apoptotic genes by eosinophils. These events combine together to cause severe lung inflammation and compromised lung immunity. Therapeutic interventions that can boost host immune response in the lungs might thus provide relief to patients with tropical pulmonary eosinophilia. *J. Leukoc. Biol.* 99: 619–628; 2016.

Introduction

TPE is a rare and serious inflammatory disorder of the lungs that is seen in a small minority of patients infected with the filarial parasites *Wuchereria bancrofti* and *Brugia malayi* [1]. Although the hypersensitive response of eosinophils due to degranulation and release of antigenic constituents of microfilariae entrapped in the lung vasculature of infected persons causes TPE, untreated TPE can lead to lung fibrosis and even death [2]. The clinical symptoms of TPE include peripheral eosinophilia, eosinophilic alveolitis, and parasite-specific IgE and IgG antibodies in serum, and lung lavage and lung biopsies of such patients show the dominance of eosinophils that correlate with the pathologic manifestations of TPE.

Although eosinophils have been a subject matter of intense investigation during helminthes infections, their study has been complicated by their relatively fragile nature and low numbers present under homeostatic conditions, making their isolation and subsequent comparisons between healthy and infected individuals extremely difficult. Moreover, the dual nature of eosinophils under different diseased conditions results in both protective and pathologic outcomes (e.g., eosinophils help in parasite killing, but activated eosinophils are injurious to the host, because they secrete many inflammatory molecules that have immunomodulatory effects on the host immune system) [3–6]. It is this behavior of eosinophils that has made the immunologic etiology of TPE very confusing and complicated [6]. However, even so, no exhaustive study has been done to identify the genes and proteins of eosinophils that play a central role in the pathogenesis of TPE.

In the present study, we developed a mouse model of TPE that exhibited cardinal features of human TPE pathogenesis

Abbreviations: AAMΦ = alternatively activated macrophages, AMΦ = alveolar macrophages, BAL = bronchoalveolar fluid, BM-mf = *Brugia malayi* microfilariae, DCs = dendritic cells, FIRE = F4/80-like receptor, FSC = forward light scatter, IMΦ = interstitial macrophages, LDCs = lymphoid dendritic cells, mDC = myeloid dendritic cells, MFI = mean fluorescence intensity, pDCs = plasmacytoid dendritic cells, TPE = tropical pulmonary eosinophilia

1. Correspondence: Parasitology Division, Council of Scientific and Industrial Research–Central Drug Research Institute, Sector 10, Jankipuram Extension, Sitapur Road, Lucknow, Uttar Pradesh 226031, India. E-mail: mrigank_srivastava@cdri.res.in

and used FACS combined with real-time RT-PCR to analyze the gene expression patterns of flow-sorted, highly purified lung eosinophils and macrophages. The results of the study showed elevated levels of eosinophil chemoattractants and Th2 cytokines in the BAL fluid and lung parenchyma of TPE mice that correlated with heavy eosinophil infiltrations and pathologic manifestations in the lungs of infected animals. FACS eosinophils from TPE mice exhibited upregulated mRNA levels of the anti-apoptotic gene, *Bcl2,* and proapoptotic genes *Bim* and *Bax* were significantly downregulated. Furthermore, AMΦ from TPE mice showed functional impairment, and lung macrophages were alternatively activated. Taken together, we show that host lung immunity is severely compromised during TPE pathogenesis; therefore, strategies that can boost the immune response in the lungs might provide relief to persons with TPE.

MATERIALS AND METHODS

Animals

Animals were procured from the national animal house facility of Council of Scientific and Industrial Research–Central Drug Research Institute and were used according to the guidelines of the institutional animal ethics committee. BALB/c mice were used to establish a mouse model of TPE, and previously infected *Meriones unguiculatus* [Mongolian jird (or gerbil)] were used for recovery of Bm-mf.

Reagents

Collagenase-1, DNase-1, MTT, Griess reagent, FITC-dextran, concanavalin-A, and mouse Ig subtyping kit were all purchased from Sigma-Aldrich (St. Louis, MO, USA). cDNA synthesis kit and SYBR green master mix were purchased from Applied Biosystems (Perkin Elmer, Forster City, CA, USA). Lymphocyte separation media were purchased from Lonza (Walkersville, MD, USA). May-Grünwald-Giemsa stain and H&E stains were purchased from Merck & Co. (Darmstadt, Germany). CD11c, F4/80, and CD4 MACS kit were purchased from Miltenyi Biotec (Bergisch-Gladbach, Germany). Trizol reagent and F4/80 anti-mouse monoclonal antibody were purchased from Invitrogen (Paisley, United Kingdom). PDCA-1 anti-mouse monoclonal antibody was purchased from eBioscience (San Diego, CA, USA). The IL-5 ELISA kit, mouse cytometric bead array kit, and all other anti-mouse monoclonal antibodies (i.e., CD11c, CD11b, CD8a, CD45, Gr-1, Siglec-F, MHC-II, and CD49d) were purchased from BD Biosciences (Heidelberg, Germany).

Development of mouse model of TPE

A mouse model of TPE was developed essentially as described previously [7]. In brief, the peritoneal cavities of previously infected gerbils were lavaged, and microfilariae were separated from contaminating leukocytes using lymphocyte separation media. The animals were separated into 3 groups. The animals in group 1 (sham infected) received PBS intravenously. The animals in group 2 received a single dose of 2×10^5 live Bm-mf (primary infection control). Finally, the animals in group 3 were first sensitized by 3 repeated subcutaneous doses of 1×10^5 frozen Bm-mf spaced 1 week apart, followed by a gap of 1 week and subsequent administration of 2×10^5 live Bm-mf. After another gap of 10 d, the animals in group 3 exhibited the typical manifestations of TPE (TPE group).

BAL fluid and estimation of cytokines

The animals were sacrificed, and BAL fluid was collected into 2 separate aliquots of 1.5 ml and 4.5 ml, as described previously [8]. Supernatant from the 1.5-ml aliquot was used for estimation of cytokines using the mouse cytometric bead array kit or ELISA, and cells from the fractions were pooled, counted, and used to estimate leukocyte differentials, as described previously [9]. In brief, BAL fluid cells from different treatment groups were cytocentrifuged at 600 rpm for 8 min, and the deposited cells were fixed and stained with May-Grünwald-Giemsa stain. Leukocytes were classified as eosinophils, neutrophils, and mononuclear cells according to the cellular staining and morphology characteristics. In each case, 200 cells were counted, and the percentage of each type of cell was calculated. The remaining BAL fluid cells were used to estimate the NO levels, phagocytosis, and T-cell proliferation capacity, as described in the subsequent sections.

Estimation of NO production, phagocytosis, and T-cell proliferation ability of AMΦ

AMΦ were isolated, as described previously [10]. In brief, BAL fluid cells were plated for 2 h in a CO_2 incubator. Thereafter, the supernatant was removed, and the adherent cells (mostly macrophages) were counted and cultured for an additional 48 h. The NO levels were estimated in the culture supernatant by Greiss reagent, as described previously [11]. For estimation of phagocytosis, AMΦ were cultured in the presence of FITC-dextran (1 mg/ml) for 2 h, and the increase in FITC fluorescence was measured using flow cytometry, as described previously [12]. For estimation of T-cell proliferation, $CD4^+$ T cells purified from the spleens of naive mice using CD4 magnetic beads were cocultured with AMΦ in the presence of concanavalin A for 48 h. Mitochondrial activity, as a measure of T-cell proliferation, was subsequently measured by MTT assay, as described previously [11].

Lung histopathologic examination

The mice were sacrificed and their lungs gently perfused with ice-cold PBS supplemented with 2 mM EDTA until visually free of blood. Next, the lungs were infused with neutral-buffered formalin, carefully excised, and immersed in formalin for 24 h at room temperature. After fixation, lungs were embedded in paraffin, sectioned into 5-μm-thick sections, and stained with H&E for assessment of the overall inflammatory response, as described previously [13].

Flow cytometry and sorting of lung eosinophils and macrophages

The mouse lungs were carefully perfused, excised, cut into small pieces, and incubated for 30 min in a digestion medium containing 2 mg/ml collagenase and 80 U/ml DNase-1. Thereafter, the digested lung tissue was processed into single cell suspension by passage through a 40-μM cell strainer. CD11c-positive cells (mostly lung macrophages and DCs) were enriched using CD11c beads, as described previously [9], and both CD11c-positive and CD11c-negative cell fractions were collected. Monoclonal antibodies directed against CD11c, CD11b, CD8a, F4/80, and PDCA-1 were used for immunophenotyping the lung leukocyte subsets present in the CD11c-positive cell fraction, and monoclonal antibodies directed against CD45, Gr-1, CD49d, CD11b, Siglec-F, and MHC-II were used for immunophenotyping the cells present in the CD11c-negative cell fraction. In a separate set of experiments, single cell lung suspensions from ≥5–6 identically treated mice were pooled and enriched using F4/80 beads. Lung eosinophils and lung macrophages were then sorted from this fraction on a high-speed FACS Aria flow cytometer (BD Biosciences) fitted with a 70-μm nozzle, as described previously [9]. In brief, flow cytometric data were acquired on 5-decade log-scale dot plots displaying FSC area vs. side scatter area to exclude contaminating dead cells and debris. A second hierarchy gate was set in FSC-A vs. FSC-H dot plot to exclude cell doublets. Thereafter, the cell populations within the FSC-A/FSC-H dot plot were segregated according to their differential expression profile of the stated markers. After sorting, the sorted cells were subjected to postsort analysis to ascertain their purity, and a small fraction was used to prepare cytospins. The remaining cells were immediately lysed in Trizol reagent to extract total cellular RNA. The details of the antibodies, their clones, and their fluorochrome specification are listed in **Table 1**.

TABLE 1. Specification of monoclonal antibodies

Antigen	Clone	Fluorochrome	Company
F4/80	BM8	Pac Blue	Invitrogen
PDCA-1	eBio927	PE	eBioscience
CD11c	HL3	FITC	BD Bioscience
CD11b	M1/70	APC	BD Bioscience
CD8a	53-6.7	PerCP Cy5.5	BD Bioscience
CD45	30-F11	PerCP	BD Bioscience
Gr-1	RB6-8C5	V450	BD Bioscience
Siglec-F	E50-2440	PE	BD Bioscience
MHC-II	2G9	FITC	BD Bioscience
CD49d	R1-2	PE	BD Bioscience

Total cellular RNA isolation, cDNA synthesis, and real-time RT-PCR

Total cellular RNA was isolated, quantified, and reverse transcribed, as described previously [8]. In brief, total cellular RNA was isolated using Trizol reagent and quantified using NanoDrop 2000 spectrophotometer (Thermo Scientific, Hudson, NH, USA). Isolated RNA was subjected to DNase-1 treatment (1 U/μg RNA) to rule out any traces of genomic DNA contamination, and only those RNA preparations exceeding $A_{260/280}$ ≥1.90 were processed for reverse transcription and real-time RT-PCR analysis. Reactions were run on an iQ5 cycler (Bio-Rad, Hercules, CA, USA) using the SYBR green master mix. β-Actin was used as the reference gene, and the mean fold changes were calculated using the $2^{-\Delta\Delta CT}$ method [14]. Primer sequences were either taken from previously published reports [15] or were designed using the Primer3 input software (http://bioinfo.ut.ee/primer3-0.4.0/). The primer sequences designed by us are listed in **Table 2**.

Statistical analysis

All data are presented as mean ± SD derived from 3 independent experiments, with ≥5–6 animals per group. Statistical analysis was performed using the Student *t* test, and $P \leq 0.05$, $P \leq 0.01$, and $P \leq 0.001$ between the different groups were considered significant, highly significant, and very highly significant, respectively.

RESULTS

TPE mice show lung eosinophilia, elevated levels of IgE and IgG in serum, and rapidly clear microfilariae from the peripheral circulation

Different groups of mice were infected as described in Materials and Methods (**Fig. 1A**). The results showed that TPE mice rapidly cleared microfilariae from the peripheral circulation by 10 d after infection compared with the primary infection control mice (Fig. 1B; $P \leq 0.001$). Also, cytospins from the BAL fluid of TPE mice showed higher leukocyte counts, with domination of eosinophils and macrophages compared with either control (Fig. 1C and D). Eosinophils constituted 30% of the total BAL fluid cell pool in the TPE mice and was about 25-fold ($P \leq 0.001$) and 7-fold ($P \leq 0.001$) greater than those in the sham-infected and primary infection control mice, respectively (Fig. 1C). Histopathologic analysis of the TPE mice lungs also revealed damaged lung architecture, thickened septa, and heavy perivascular and peribronchiolar leukocytic infiltrations, which were absent in either control group (Fig. 1D). Elevated titers of IgE, IgG1, IgG2a, IgG2b, and IgG3 were also noted in the serum of TPE mice (Fig. 1E and F). Overall, these results show that infection with live Bm-mf alone does not cause pathologic manifestations in the lungs; however, sensitization with Bm-mf, followed by administration of live microfilariae, led to the development of TPE [6].

Eosinophil chemoattractants and Th2 cytokines dominate lung cytokine milieu in TPE mice

AMΦ from TPE mice showed elevated transcript levels of Th2 cytokines IL-4 ($P \leq 0.01$) and IL-5 ($P \leq 0.05$), along with the eosinophil chemoattractant CCL11 ($P \leq 0.01$) and the monocyte chemoattractant CCL2 ($P \leq 0.05$). The levels of Th1 cytokine IL-12 decreased significantly ($P \leq 0.001$) compared with those in the primary infection control mice (**Fig. 2A**). Similarly, the lung parenchymal cells from the TPE mice showed significantly upregulated levels of IL-4 ($P \leq 0.01$), IL-5 ($P \leq 0.05$), and CCL11 ($P \leq 0.01$), and the levels of IL-12 were downregulated ($P \leq 0.01$). Low expression levels of IL-10 ($P \leq 0.05$), CCL-2 ($P \leq 0.05$), and CCL-5 ($P \leq 0.01$) were observed in the TPE mice compared with the levels in the primary infection control mice. However, no significant differences were observed in the expression levels of the other mediators studied (Fig. 2B). We validated these findings at the protein level and found that changes at the transcript level were largely preserved (**Fig. 3**). Although the levels of the proinflammatory cytokines IL-6, TNF-α, and IFN-γ were significantly higher in the primary infection control mice ($P \leq 0.001$), we did not observe any major change in the level of IL-17. These results suggested domination of eosinophil chemoattractants and Th2 cytokine milieu in the lungs of the TPE mice.

Neutrophils and eosinophils increase in the lungs of TPE mice

Immunophenotyping of the leukocyte subsets present in the lungs of mice from different treatment groups was performed using a combination of different surface markers, as described previously [16, 17]. Lung DCs and macrophages were identified in the CD11c-positive fraction, and eosinophils were identified in the CD11c depleted fraction, as described previously [18]. Our results revealed significantly reduced percentages of AMΦ ($CD11c^{hi}$, $F4/80^{pos}$), plasmacytoid DCs ($CD11c^{mid}$, $PDCA\text{-}1^{pos}$), lymphoid DCs ($CD11c^{pos}$, $CD11b^{neg}$, $CD8a^{pos}$), resident monocytes ($CD45^{pos}$, $Gr1^{neg}$, $CD49d^{pos}$), and inflammatory monocytes ($CD45^{pos}$, $Gr1^{mid}$, $CD49d^{pos}$) in the lungs of TPE mice (**Fig. 4A–C**). The percentages of IMΦ ($CD11c^{mid}$, $F4/80^{pos}$), neutrophils ($CD45^{pos}$, $Gr1^{hi}$, $CD49d^{lo/mid}$), and eosinophils ($CD45^{pos}$, $Gr1^{low}$, $CD49d^{o/mid}$, $CCR3^{hi}$) increased compared with the levels in the sham-infected and primary infection control mice (Fig. 4A–C). However, no major change was seen in the percentage of myeloid DCs ($CD11c^{pos}$, $CD11b^{hi}$, $CD8a^{neg}$, Fig. 4A–C) among the different groups. Eosinophils from the TPE mice showed downregulation of surface receptor CCR-3 (Fig. 4B; $P \leq 0.05$ between the TPE and sham infected groups and $P \leq 0.001$ between the TPE and primary infection control groups). Taken together, these results show impaired trafficking of major APCs in the lungs of TPE mice, and reduced percentages of AMΦ might result from the early apoptosis of these cells, as reported previously [19–21].

TABLE 2. Primer sequences used for real-time RT-PCR

Sr. No.	Gene	Forward primer (5′-3′)	Reverse primer (5′-3′)
1	IL-10	GCTCTTACTGACTGGCATGAG	CGCAGCTCTAGGAGCATGTG
2	IL-12	CTCAGGATCGCTATTACAATTCCT	TTCCAACGTTGCATCCTAGGATC
3	CCL2	TTAAAAACCTGGATCGGAACCAA	GCATTAGCTTCAGATTTACGGGT
4	CCL5	TGCCTCACCATATGGCTCGG	GGACTAGAGCAAGCGATGAC
5	CCL11	GCAGAGCTCCACAGCGCTTC	AGTCCTTGGGCGACTGGTGT
6	CCL24	GCTCTGCTACGATCGTTG	AGCAAACTTGGTTCTCACTG
7	ARG-1	GTATGACGTGAGAGACCACG	CTCGCAAGCCAATGTA
8	NOS-2	GTTCTCAGCCCAACAATACAAGA	GTGGACGGGTCGATGTCAC
9	FIZZ-1	CCAATCCAGCTAACTATCCCTCC	ACCCAGTAGCAGTCATCCCA
10	YM-1	CAGGTCTGGCAATTCTTCTGAA	GTCTTGCTCATGTGTGTAAGTGA
11	MBP	GAGCGTCTGCTCTTCATCTG	GAACTTCCATCAACCCATCG
12	FCNA	GGAGAAAGGCGATACAGGAG	TTGGACTGGTGGCAGTTGTG
13	EPX	CATACATGAAGGTGGCATCG	CTCTCGAAACCGTGGTGATG
14	FIRE	CTGGAATGCTGCTTATCTGGTC	GACATTTCTCATGGGGCTCAAT
15	Bcl-2	ATGCCTTTGTGGAACTATATGGC	GGTATGCACCCAGAGTGATGC
16	Bim	CCCGGAGATACGGATTGCAC	GCCTCGCGGTAATCATTTGC
17	Bax	TGAAGACAGGGGCCTTTTTG	AATTCGCCGGAGACACTCG
18	TLR-1	TGAGGGTCCTGATAATGTCCTAC	AGAGGTCCAAATGCTTGAGGC
19	TLR-2	CACCACTGCCCGTAGATGAAG	AGGGTACAGTCGTCGAACTCT
20	TLR-3	GTGAGATACAACGTAGCTGACTG	TCCTGCATCCAAGATAGCAAGT
21	TLR-4	ATGGCATGGCTTACACCACC	GAGGCCAATTTTGTCTCCACA
22	TLR-5	GCAGGATCATGGCATGTCAAC	ATCTGGGTGAGGTTACAGCCT
23	TLR-6	TGAGCCAAGACAGAAAACCCA	GGGACATGAGTAAGGTTCCTGTT
24	TLR-7	ATGTGGACACGGAAGAGACAA	GGTAAGGGTAAGATTGGTGGTG
25	TLR-8	GAAAACATGCCCCCTCAGTCA	CGTCACAAGGATAGCTTCTGGAA
26	TLR-9	ATGGTTCTCCGTCGAAGGACT	GAGGCTTCAGCTCACAGGG

AMΦ are functionally impaired during TPE pathogenesis

AMΦ are the main phagocytic cells in the lungs and play a central role in the regulation of eosinophilia [22]. AMΦ from TPE mice displayed impaired phagocytosis, which was evident by reduced uptake of FITC-labeled dextran beads (MFI 39.13 ± 2.84) compared with the sham-infected (MFI 52.9 ± 2.47) and primary infection control (MFI 46.60 ± 3.47) mice (**Fig. 5A**; $P \leq 0.05$ for both comparisons). Furthermore, they showed a significantly reduced NO production capacity (Fig. 5B; $P \leq 0.001$ between the TPE and sham-infected groups and $P \leq 0.01$ between the TPE and primary infection control groups) and drastically attenuated T-cell proliferation capacity (Fig. 5C; $P \leq 0.01$ between the TPE and sham-infected groups and $P \leq 0.05$ between the TPE and primary infection control groups), signifying their complete functional impairment during TPE pathogenesis.

Eosinophils from TPE mice upregulate anti-apoptotic gene, and lung macrophages are alternatively activated

Lung eosinophils ($CD45^{pos}$, MHC II^{neg}, Siglec F^{pos}) and lung macrophages ($CD45^{hi}$, MHC II^{pos}, Siglec F^{pos}) were sorted from mice of different treatment groups, as described in Materials and Methods. The postsort analysis and May-Grünwald-Giemsa–stained cytospin preparations of sorted cells confirmed their very high purity (≥98%; **Fig. 6A**). Real-time RT-PCR analysis of flow-sorted eosinophils from TPE mice showed significantly upregulated levels of ficolin A ($P \leq 0.01$), a secretary protein, and the levels of FIRE ($P \leq 0.01$) and inhibitory tyrosine receptors ($P \leq 0.001$; Axl) were heavily downregulated (Fig. 6B). Eosinophils from TPE mice upregulated Bcl-2, a key anti-apoptotic gene, and the proapoptotic genes, *Bim* ($P \leq 0.05$) and *Bax* ($P \leq 0.01$), were significantly downregulated (Fig. 6B). No significant differences were, however, observed in the expression levels of other eosinophil proteins studied (Fig. 6B).

Similarly, flow-sorted macrophages from TPE mice upregulated the key alternative activation marker, Arginase-1 ($P \leq 0.05$), and eosinophil chemotactic proteins Ym-1 ($P \leq 0.05$) and FIZZ-1 ($P \leq 0.01$). However, the classic activation marker, NOS-2, was significantly downregulated ($P \leq 0.05$; Fig. 6C). These results showed alternative activation of lung macrophages in TPE mice. Similarly, lung macrophages from TPE mice significantly upregulated the levels of TLR-2 and TLR-6 (Fig. 6D; $P \leq 0.01$ for both). However, the levels of TLR-4 and TLR-7 were significantly downregulated (Fig. 6D; $P \leq 0.01$ for both). Quite interestingly, TLR-3 was upregulated in the primary infection control mice (Fig. 6D; $P \leq 0.01$), but no significant differences were observed in the other TLRs studied.

DISCUSSION

The exact mechanism behind the pathogenesis of TPE is not clear; however, the heavy influx of eosinophils into the lungs of TPE patients is believed to contribute to the pathologic features of TPE, much the same as eosinophils have been implicated in the pathogenesis of many other allergic diseases [22–26]. However, no exhaustive study has been done to identify the genes and proteins of eosinophils that might be responsible for

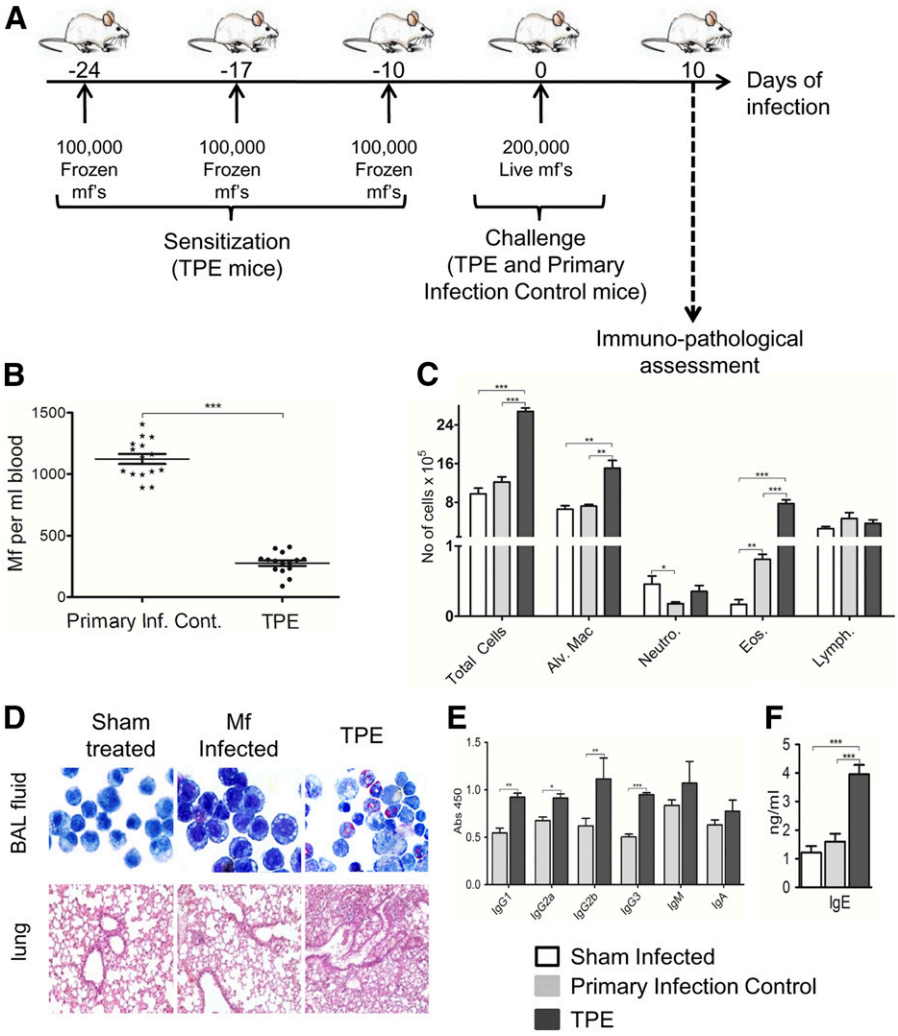

Figure 1. Mouse model of TPE. (A) Schematic representation of the animal treatment protocol for establishment of the mouse model of TPE. BALB/c mice were infected with either live BM-mf (primary infection control) or sensitized and challenged with BM-mf (TPE mice) at indicated time points. Immunologic studies were performed as described in Materials and Methods. (B) Comparison of microfilariae (mf) counts in the blood of primary infection control and TPE mice. (C) Total and differential leukocyte counts in different groups of infected mice. (D) May-Grünwald-Giemsa–stained cytospins from BAL fluid (upper) and H&E–stained lung sections (lower) of mice lungs from different groups of infected mice. (E and F) Concentration of parasite-specific IgE and IgG subtypes, IgM, and IgA in sera of mice from different treatment groups. Data are representative of 3 independent experiments with 5–6 mice per group. $*P \leq 0.05$, $**P \leq 0.01$, and $***P \leq 0.001$ was considered significant, highly significant, and very highly significant, respectively.

the TPE pathogenesis. Although eosinophils increase under allergic and inflammatory conditions, they are often accompanied by other contaminating leukocytes, making their isolation and comparisons between homeostatic and diseased conditions extremely difficult.

In the present study, we used FACS combined with real-time RT-PCR to study the changes in the gene expression patterns of the flow-sorted lung eosinophils and macrophages in a mouse model of TPE. In addition, we performed immunophenotyping studies of the different leukocyte subsets present in the lungs of TPE mice and investigated the role of AMΦ during TPE pathogenesis. We compared our results with those from sham-infected mice that had received PBS and primary infection control mice that had received only live microfilariae. The rationale behind using 2 different controls was that although the TPE mice represented a pathologic condition, the sham-infected and primary infection control mice represented the homeostatic and nonpathologic setting, respectively, which helped us in understanding and comparing the gene expression profile of eosinophils under 3 different conditions. This comparative rationale finds resonance in an earlier work by Cadman et al. [6], who showed that eosinophils offer protection during primary infection with Bm-mf, and their activation during a secondary challenge (eg, in the case of TPE) results in injurious lung pathologic features.

In the present study, TPE mice exhibited peripheral eosinophilia, eosinophilic alveolitis, and elevated titers of IgE and IgG subtypes in the serum, in agreement with previous reports [7]. Moreover, eosinophils from TPE mice downregulated surface expression of CCR3, which is responsible for differentiation and activation of eosinophils during inflammatory processes [27]. Higher expression of CCL-5 and CCL-11 during TPE could be responsible for CCR-3 downregulation, because CCR-3 internalization has been reported after prolonged exposure of eosinophils with CCR-3 ligands [28]. Also, studies have reported that IL-3–mediated downregulation of CCR-3 in human eosinophils [29]. Thus, the exact role of CCR-3 during TPE pathogenesis needs evaluation. Because the cytokine milieu helps in determining the immunologic etiology of any disease [30], we elucidated the prevailing cytokine milieu in the lungs of TPE mice. Our results showed elevated levels of eosinophil chemoattractants, IL-5 and CCL11, in the lungs of TPE mice. This is an important finding, because CCL-11 has been shown to interact with CCR-3, thereby promoting maturation, activation, and

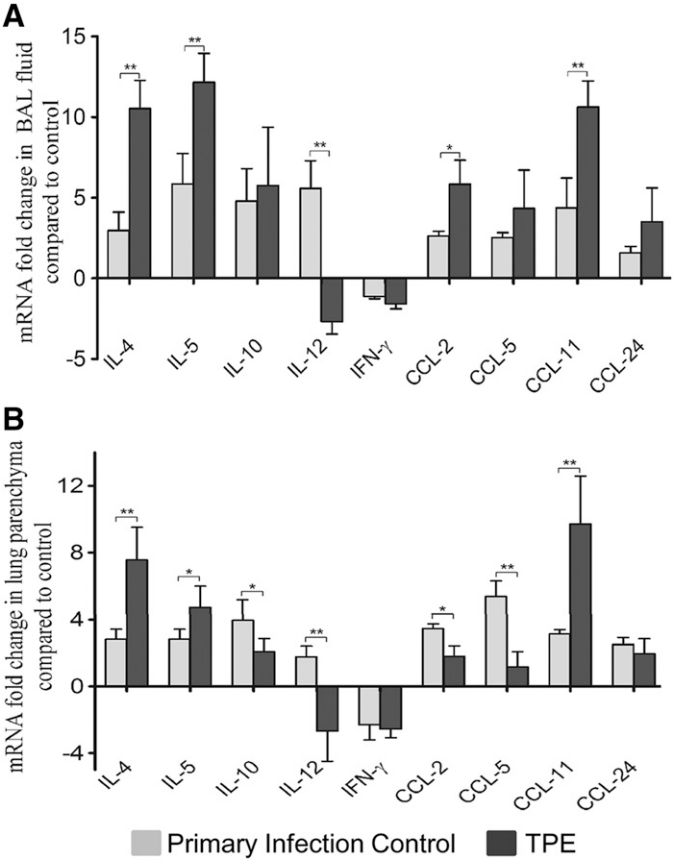

Figure 2. mRNA expression profile of cytokines. Real-time RT-PCR was used to measure the transcript levels of the different cytokines present in (A) BAL fluid and (B) lung parenchyma of different groups of infected mice. Data are representative of 3 independent experiments with 5–6 mice per group. $*P \leq 0.05$, $**P \leq 0.01$, and $***P \leq 0.001$ was considered significant, highly significant, and very highly significant, respectively.

differentiation of eosinophils [27]. Also, previous studies of CCL-11 KO mice have shown drastically reduced eosinophil counts and alleviated airway hyperresponsiveness, highlighting the importance of CCL11 and CCR3 interactions [31]. Similarly, elevated levels of Th2 cytokines and the presence of AAMΦ, such as were observed in the present study, could be additional factors responsible for promoting pulmonary eosinophilia. Previous studies have documented reversal of pathologic symptoms in mice after attenuation of Th2 cytokines [32, 33]. AAMΦ have been shown to aid in the recruitment of eosinophils from the peripheral circulation [25].

Surprisingly, monocyte recruitment was hampered in TPE mice despite increased transcript levels of the monocyte chemoattractant, CCL2, in their BAL fluid. This was an unexpected finding, because CCL2 has been shown to exert its protective role in the activation of macrophages and induction of eosinophilia [34]. However, this observation could have resulted from either filaria-induced monocyte dysfunction [35, 36], or induction of a regulatory monocyte/macrophage phenotype which suppresses innate and adaptive immune responses in *B. malayi*–infected animals [37]. However, as expected, reduced monocyte counts corroborated with reduced AMΦ in the lungs of TPE mice, which might have resulted from either impaired differentiation of monocytes into macrophages or early apoptosis of macrophages during filarial infection. Although we did not directly address the apoptosis issue in the present study, previous reports have documented the role of caspases in causing apoptosis during filarial infection [19]. Moreover, it is important to reconcile the findings from Semnani et al. [20]. They showed that *B. malayi* contains a homolog of human macrophage inhibitory factor, which activates monocytes and macrophages to produce IL-8 and TNF-α. This suggests that parasite-derived products also serve to induce indirect apoptosis through induction of cytokines and chemokines [20]. Finally, we believe that apoptosis of macrophages could also have resulted from microfilaria-induced cell death, a key feature seen during TPE pathogenesis [21].

We also observed rapid clearance of microfilariae from the peripheral circulation of the TPE mice. This signifies 2 points. First, this indicates entrapment of microfilariae into the pulmonary vasculature of these animals. Second, it highlights an important correlation with the hypersensitive response, as reported previously [6, 38]. The results of the present study also yielded interesting insights into the functional status of AMΦ in TPE mice. Our findings showed considerable functional impairment, which was evident by their reduced phagocytosis capacity, drastically attenuated NO release capacity, and an inability to cause T-cell proliferation. Also, flow-sorted, and thus highly purified, lung macrophages exhibited an alternatively activated profile, with downregulated NOS and elevated Arg-1, Ym-1, and FIZZ-1 transcription levels. These findings are interesting, because classically activated macrophages not only eliminate airway hyperresponsiveness but also offer protection against many pathogens [39]. Also, AAMΦ help in helminth survival and cause pulmonary eosinophilia [25, 40]. Similarly, IMΦ, which

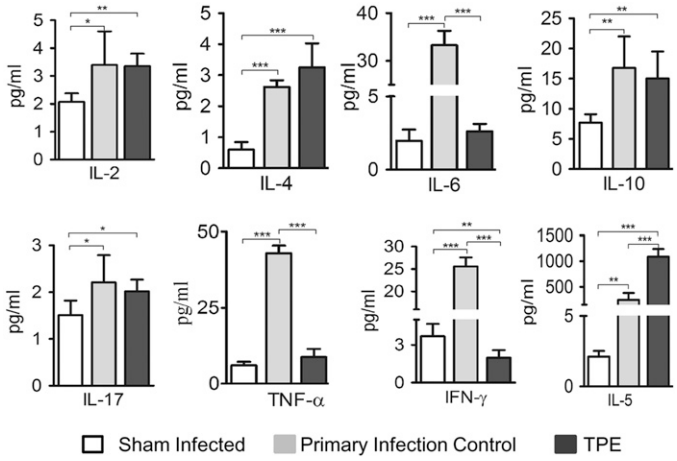

Figure 3. Concentration of different cytokines. Mouse cytometric bead assay kit or ELISA was used to measure concentrations of different cytokines present in the BAL fluid of different groups of infected mice. Data are representative of 3 independent experiments with 5–6 mice per group. $*P \leq 0.05$, $**P \leq 0.01$, and $***P \leq 0.001$ was considered significant, highly significant, and very highly significant, respectively.

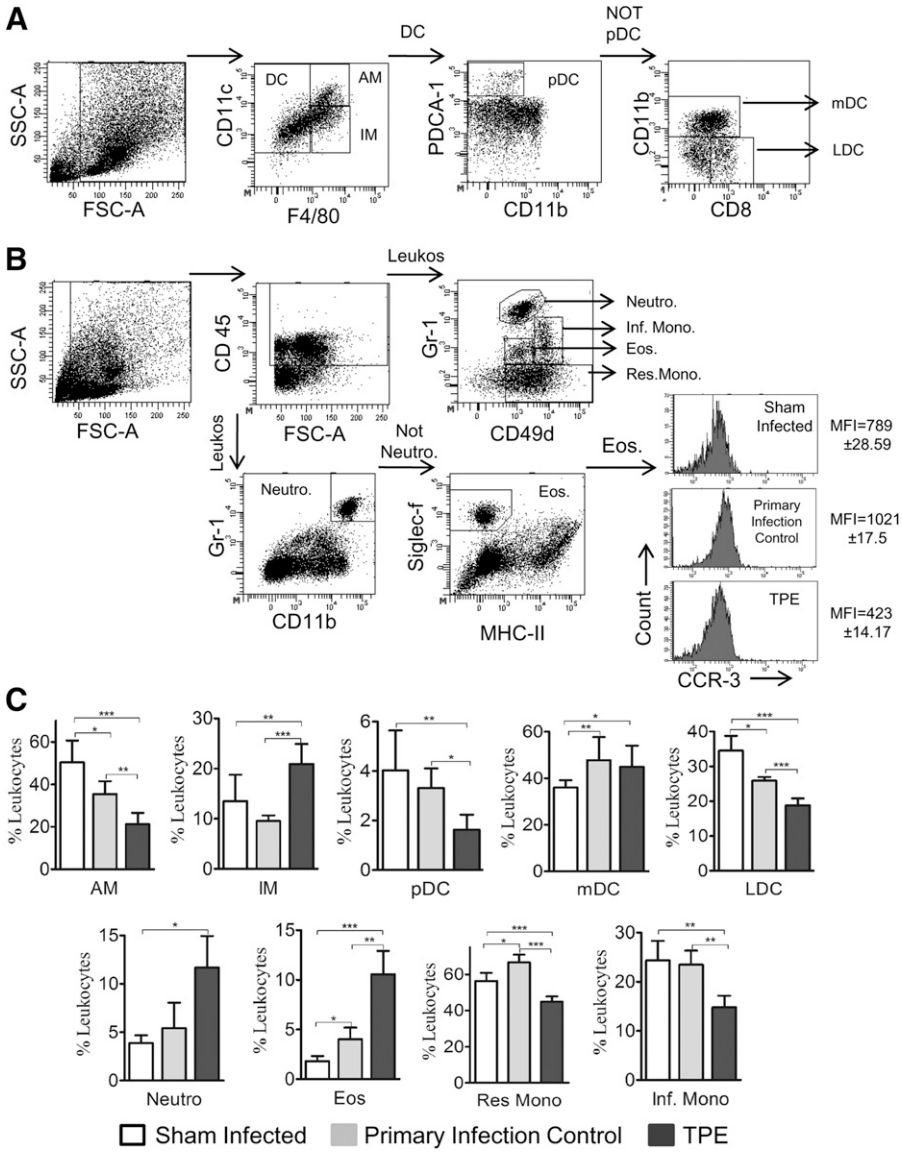

Figure 4. Identification of different leukocyte subsets present in the lungs of mice. (A) Gating strategy for identification of DC and macrophage subsets present in the CD11c-positive cell fraction of mice from different treatment groups. (B) Gating strategy for identification of neutrophils, eosinophils, resident, and inflammatory monocytes present in the CD11c-negative cell fraction of mice from different treatment groups. (C) Percentages of respective respiratory leukocyte subsets present in the lung digests of mice from different treatment groups. Data are representative of 3 independent experiments, with ≥ 5–6 animals per group. $*P \leq 0.05$, $**P \leq 0.01$, and $***P \leq 0.001$ was considered significant, highly significant, and very highly significant, respectively. AM = alveolar macrophages, DC = dendritic cells, Eos = eosinophils, IM = interstitial macrophages, Inf. Mono = inflammatory monocytes, LDC = lymphoid dendritic cells, Neutro = neutrophils, pDC = plasmacytoid dendritic cells, Res. Mono. = resident monocytes.

help in maintaining lung homeostasis, were increased in the lungs of TPE mice. This might have resulted from the prevailing inflammatory conditions in the lungs, because these cells exaggerate pulmonary inflammation, thereby contributing toward the pathologic manifestations observed during TPE [41, 42]. Taken together, these findings are novel, especially in the context of exploring the therapeutic potential of alternative activation pathways of macrophages, because the functional adaptivity of macrophages allows for reversal of phenotypes with proinflammatory stimuli that can be used for therapeutic benefits [23].

Among the other leukocyte subset studied, neutrophils increased in the lungs of the TPE mice. This might have resulted from the degenerating *Wolbachia* present inside the microfilariae, which releases neutrophil chemoattractants [43], or the presence of monocytes, which help in alveolar neutrophil emigration during inflammatory conditions [44]. Also, the contribution of increased expression of TLR-2 on macrophages cannot be ruled out, because increased TLR2 expression has been implicated in neutrophil recruitment during hypersensitivity pneumonitis [45]. Similarly, reduced percentages of plasmacytoid DCs and lymphoid DCs, but not myeloid DCs, in the lungs of TPE mice could be a result of either microfilaria-induced death of APCs, as reported previously [46], or a microfilaria-induced inflammatory response, because pDCs have been shown to induce regulatory T cells in the lungs that aid in allergen-specific tolerance [47, 48]. However, it is important to note that although the exact mechanism of parasite-induced cell death is still a matter of investigation, what is clear, is that neither Fas/FasL expression nor NO activation of caspases underlies the apoptosis seen in APCs [19]. Also, even those DCs that remain alive are functionally impaired to produce inflammatory cytokines [46]. Furthermore, downregulation of lymphoid DCs can be linked to type 2 immunity during TPE pathogenesis, because they have been reported to induce a Th1 response in a mouse model [49]. pDCs have been shown to exhibit a regulatory role and drive a

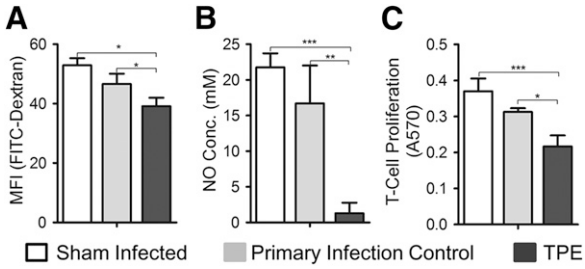

Figure 5. Assessment of AMΦ functions. (A) Measurement of phagocytosis capacity of AMΦ after incubation with FITC-Dextran. (B) Estimation of NO production by macrophages. (C) Estimation of T-cell proliferation capacity of AMΦ after coculturing with CD4+ T cells. Data are representative of 3 independent experiments, with ≥5–6 animals per group. $*P \leq 0.05$, $**P \leq 0.01$, and $***P \leq 0.001$ was considered significant, highly significant, and very highly significant, respectively.

potent Th1 polarization both in vitro and in vivo [50]. However, some contradictory studies have reported that pDCs induce Th2 polarization of allogeneic naive T cells [51]; thus, their exact role in T-cell polarization during TPE pathogenesis needs to be evaluated in greater detail.

Considering the importance of TLRs in sensing pathogen-associated molecular patterns, we investigated the expression patterns of TLRs in flow-sorted lung macrophages and found selective upregulation of TLR-2 and TLR-6, with subsequent downregulation of TLR-4 and TLR-7. This is important, because downregulation of TLR-4 has been correlated with AAMΦ [52], and TLR-2–dependent functional anarchy of AMΦ has been reported during a secondary challenge with *B. malayi* [53].

Finally, flow-sorted lung eosinophils from TPE mice revealed significantly upregulated levels of ficolin A, a lectin molecule involved in the activation of complement pathways, which aids in parasite killing [54, 55]. However, other eosinophil surface receptors (i.e., Axl and FIRE) were significantly downregulated. This finding is significant, because Axl is not only upregulated during maturation and activation of eosinophils in the lungs [25, 56], but previous studies have also documented the potential involvement of Axl in the removal of apoptotic cells under inflammatory conditions. The absence of Axl and the down-regulation of FIRE have been reported during infection with other helminths, where they exaggerate inflammatory conditions in the lung [25, 57]. Furthermore, we also evaluated the key gene of the intrinsic apoptotic pathways and found that *Bcl-2*, a key

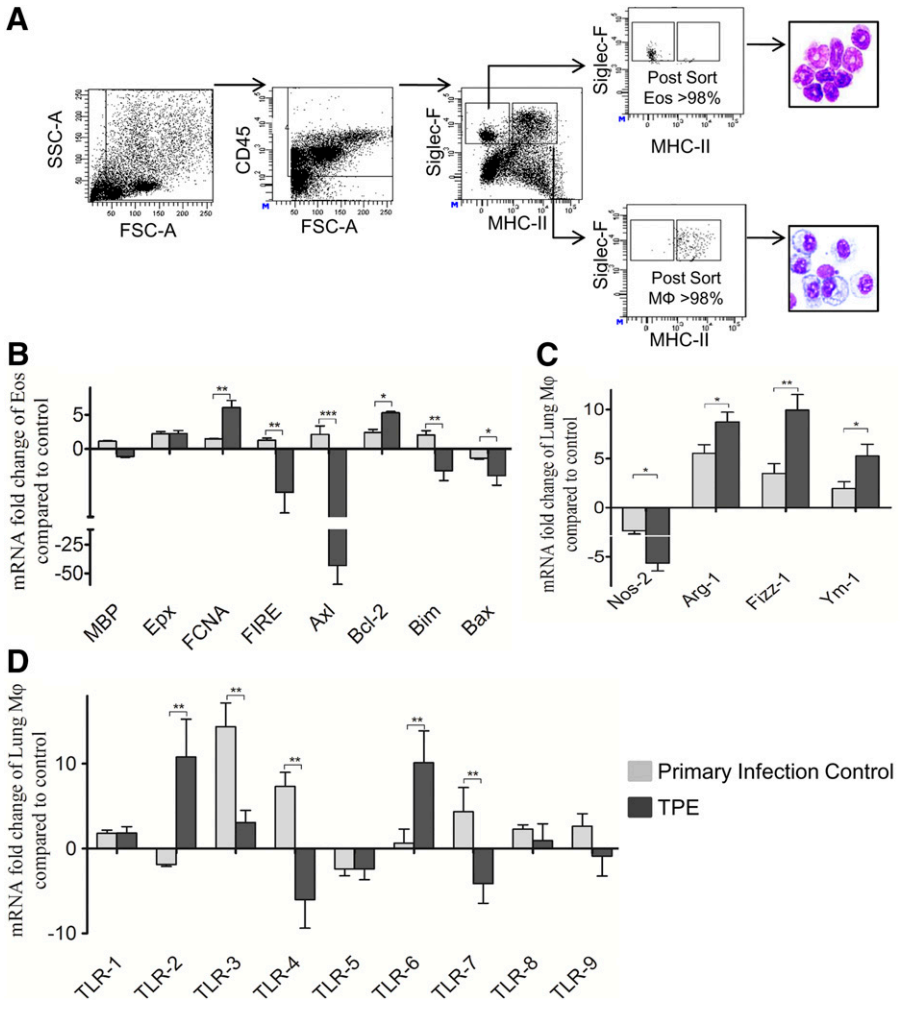

Figure 6. Sorting of lung eosinophils and macrophages and assessment of their gene expression profile. (A) Gating strategy for identification of lung eosinophils and macrophages present in F4/80-enriched lung digests of mice from different treatment groups. Postsort dot pots and May-Grünwald-Giemsa–stained cytospins illustrate very high purity (≥98%) of sorted cells. (B) mRNA expression level of cell surface markers and apoptotic and anti-apoptotic genes present in flow-sorted eosinophils. (C) mRNA expression level of classic and alternative activation markers present in purified lung macrophages. (D) mRNA expression level of different TLRs present in purified lung macrophages. Data are representative of 3 independent experiments, with 5–6 mice per group. $*P \leq 0.05$, $**P \leq 0.01$, and $***P \leq 0.001$ was considered significant, highly significant, and very highly significant, respectively.

anti-apoptotic gene, was upregulated in eosinophils, along with significantly downregulated levels of the proapoptotic genes *Bim* and *Bax*. This result was along expected lines, because Bcl proteins have been shown to delay apoptosis in eosinophils [58]. This means that eosinophils, by doing so, stayed longer in the inflamed lungs of TPE mice without becoming phagocytosed and, therefore, were able to release excessive amounts of cytosolic proteins, contributing to TPE pathogenesis. The prolonged survival of eosinophils in the airways is maintained by Th2 cytokines and is supported by the neutralization of IL-4 and IL-5, which leads to eosinophils apoptosis and alleviates pathogenesis in the mice model [59, 60]. In TPE patients, eosinophilia is also driven by Th2 cytokines, and the clinical relevance of the present study is supported by the similar behavior of human eosinophils in the presence of GM-CSF, IL-3, and IL-5 [59, 60]. Furthermore, anti-inflammatory drugs such as glucocorticoids and leukotriene antagonists promote eosinophil apoptosis and alleviate asthmatic symptoms in patients, strengthening the hypothesis that anti-apoptotic genes play an important role in the pathogenesis of TPE [61, 62].

In conclusion, we have shown that the pathogenesis of TPE is marked by functional impairment of AMΦ, alternative activation of lung macrophages, and upregulation of anti-apoptotic genes by eosinophils. Together, these events compromise host lung immunity and contribute to exaggerated pathologic manifestations in the lungs. A deeper understanding of the immunomodulatory roles of eosinophils is clearly needed, because targeting the eosinophil apoptosis pathway can boost host lung immunity, which could be beneficial to patients experiencing the filarial manifestations of TPE.

AUTHORSHIP

P.S. and M.S. conceived and designed the experiments. P.S., A.S., and M.S. performed the experiments. M.S. and A.L.V. helped with cell sorting. P.S., P.K.A., and S.S. performed lung histopathologic examinations. P.S. and M.S. analyzed the data. M.S. contributed reagents, materials, and analysis tools. P.S. and M.S. wrote the report.

ACKNOWLEDGMENTS

This work was supported by grants provided under the Council of Scientific and Industrial Research (CSIR)-Network project "new approaches towards understanding of disease dynamics and to accelerate drug discovery (UNDO)" and "Emerging and re-emerging challenges in infectious diseases: systems based drug design for infectious diseases (SPLenDID)" to M.S. The funders had no role in the study design, data collection, analysis, decision to publish, or preparation of the manuscript. The authors thankfully acknowledge the excellent technical support provided by Shikha Mishra and O.P. Yadav for maintaining *B. malayi* infection in the laboratory. P.S. and A.S. thankfully acknowledge fellowship support from the University Grants Commission and Council of Scientific and Industrial Research, New Delhi, respectively. This is CSIR-CDRI Communication number 9090.

DISCLOSURES

The authors declare no conflicts of interest.

REFERENCES

1. Ong, R. K., Doyle, R. L. (1998) Tropical pulmonary eosinophilia. *Chest* **113,** 1673–1679.
2. Boggild, A. K., Keystone, J. S., Kain, K. C. (2004) Tropical pulmonary eosinophilia: a case series in a setting of nonendemicity. *Clin. Infect. Dis.* **39,** 1123–1128.
3. Simons, J. E., Rothenberg, M. E., Lawrence, R. A. (2005) Eotaxin-1-regulated eosinophils have a critical role in innate immunity against experimental *Brugia malayi* infection. *Eur. J. Immunol.* **35,** 189–197.
4. Trivedi, S. G., Lloyd, C. M. (2007) Eosinophils in the pathogenesis of allergic airways disease. *Cell. Mol. Life Sci.* **64,** 1269–1289.
5. Hogan, S. P., Rosenberg, H. F., Moqbel, R., Phipps, S., Foster, P. S., Lacy, P., Kay, A. B., Rothenberg, M. E. (2008) Eosinophils: biological properties and role in health and disease. *Clin. Exp. Allergy* **38,** 709–750.
6. Cadman, E. T., Thysse, K. A., Bearder, S., Cheung, A. Y., Johnston, A. C., Lee, J. J., Lawrence, R. A. (2014) Eosinophils are important for protection, immunoregulation and pathology during infection with nematode microfilariae. *PLoS Pathog.* **10,** e1003988.
7. Mehlotra, R. K., Hall, L. R., Haxhiu, M. A., Pearlman, E. (2001) Reciprocal immunomodulatory effects of gamma interferon and interleukin-4 on filaria-induced airway hyperresponsiveness. *Infect. Immun.* **69,** 1463–1468.
8. Srivastava, M., Jung, S., Wilhelm, J., Fink, L., Bühling, F., Welte, T., Bohle, R. M., Seeger, W., Lohmeyer, J., Maus, U. A. (2005) The inflammatory versus constitutive trafficking of mononuclear phagocytes into the alveolar space of mice is associated with drastic changes in their gene expression profiles. *J. Immunol.* **175,** 1884–1893.
9. Srivastava, M., Meinders, A., Steinwede, K., Maus, R., Lucke, N., Bühling, F., Ehlers, S., Welte, T., Maus, U. A. (2007) Mediator responses of alveolar macrophages and kinetics of mononuclear phagocyte subset recruitment during acute primary and secondary mycobacterial infections in the lungs of mice. *Cell. Microbiol.* **9,** 738–752.
10. Zhang, X., Goncalves, R., Mosser, D. M. (2008) The isolation and characterization of murine macrophages. *Curr. Protoc. Immunol.* Chapter 14, Unit 14 1.
11. Bhardwaj, J., Siddiqui, A. J., Goyal, M., Prakash, K., Soni, A., Puri, S. K., Srivastava, M. (2015) Host immune response is severely compromised during lethal *Plasmodium vinckei* infection. *Parasitol. Res.* **114,** 3445–3457.
12. Wang, J., Yao, Y., Xiong, J., Wu, J., Tang, X., Li, G. (2015) Evaluation of the inflammatory response in macrophages stimulated with exosomes secreted by *Mycobacterium avium*-infected macrophages. *BioMed Res. Int.* **2015,** 658421.
13. Singh, V. K., Srivastava, M., Dasgupta, A., Singh, M. P., Srivastava, R., Srivastava, B. S. (2014) Increased virulence of *Mycobacterium tuberculosis* H37Rv overexpressing LipY in a murine model. *Tuberculosis (Edinb.)* **94,** 252–261.
14. Livak, K. J., Schmittgen, T. D. (2001) Analysis of relative gene expression data using real-time quantitative PCR and the 2(-Delta Delta C(T)) method. *Methods* **25,** 402–408.
15. Babayan, S. A., Attout, T., Harris, A., Taylor, M. D., Le Goff, L., Vuong, P. N., Rénia, L., Allen, J. E., Bain, O. (2006) Vaccination against filarial nematodes with irradiated larvae provides long-term protection against the third larval stage but not against subsequent life cycle stages. *Int. J. Parasitol.* **36,** 903–914.
16. Zaynagetdinov, R., Sherrill, T. P., Kendall, P. L., Segal, B. H., Weller, K. P., Tighe, R. M., Blackwell, T. S. (2013) Identification of myeloid cell subsets in murine lungs using flow cytometry. *Am. J. Respir. Cell Mol. Biol.* **49,** 180–189.
17. Hackstein, H., Wachtendorf, A., Kranz, S., Lohmeyer, J., Bein, G., Baal, N. (2012) Heterogeneity of respiratory dendritic cell subsets and lymphocyte populations in inbred mouse strains. *Respir. Res.* **13**, 94.
18. Stevens, W. W., Kim, T. S., Pujanauski, L. M., Hao, X., Braciale, T. J. (2007) Detection and quantitation of eosinophils in the murine respiratory tract by flow cytometry. *J. Immunol. Methods* **327,** 63–74.
19. Kim, P. K., Kwon, Y. G., Chung, H. T., Kim, Y. M. (2002) Regulation of caspases by nitric oxide. *Ann. N. Y. Acad. Sci.* **962,** 42–52.
20. Semnani, R. T., Nutman, T. B. (2004) Toward an understanding of the interaction between filarial parasites and host antigen-presenting cells. *Immunol. Rev.* **201,** 127–138.
21. Mathie, S. A., Dixon, K. L., Walker, S. A., Tyrrell, V., Mondhe, M., O'Donnell, V. B., Gregory, L. G., Lloyd, C. M. (2015) Alveolar macrophages are sentinels of murine pulmonary homeostasis following inhaled antigen challenge. *Allergy* **70,** 80–89.
22. Manabe, K., Nishioka, Y., Kishi, J., Inayama, M., Aono, Y., Nakamura, Y., Ogushi, F., Bando, H., Tani, K., Sone, S. (2005) Elevation of macrophage-derived chemokine in eosinophilic pneumonia: a role of alveolar macrophages. *J. Med. Invest.* **52,** 85–92.
23. Mylonas, K. J., Nair, M. G., Prieto-Lafuente, L., Paape, D., Allen, J. E. (2009) Alternatively activated macrophages elicited by helminth infection can be reprogrammed to enable microbial killing. *J. Immunol.* **182,** 3084–3094.

24. Tachimoto, H., Burdick, M. M., Hudson, S. A., Kikuchi, M., Konstantopoulos, K., Bochner, B. S. (2000) CCR3-active chemokines promote rapid detachment of eosinophils from VCAM-1 in vitro. *J. Immunol.* **165,** 2748–2754.
25. Voehringer, D., van Rooijen, N., Locksley, R. M. (2007) Eosinophils develop in distinct stages and are recruited to peripheral sites by alternatively activated macrophages. *J. Leukoc. Biol.* **81,** 1434–1444.
26. Takatsu, K., Nakajima, H. (2008) IL-5 and eosinophilia. *Curr. Opin. Immunol.* **20,** 288–294.
27. Lamkhioued, B., Abdelilah, S. G., Hamid, Q., Mansour, N., Delespesse, G., Renzi, P. M. (2003) The CCR3 receptor is involved in eosinophil differentiation and is up-regulated by Th2 cytokines in CD34+ progenitor cells. *J. Immunol.* **170,** 537–547.
28. Zimmermann, N., Conkright, J. J., Rothenberg, M. E. (1999) CC chemokine receptor-3 undergoes prolonged ligand-induced internalization. *J. Biol. Chem.* **274,** 12611–12618.
29. Dulkys, Y., Kluthe, C., Buschermöhle, T., Barg, I., Knöss, S., Kapp, A., Proudfoot, A. E., Elsner, J. (2001) IL-3 induces down-regulation of CCR3 protein and mRNA in human eosinophils. *J. Immunol.* **167,** 3443–3453.
30. Kouro, T., Takatsu, K. (2009) IL-5- and eosinophil-mediated inflammation: from discovery to therapy. *Int. Immunol.* **21,** 1303–1309.
31. Rothenberg, M. E., MacLean, J. A., Pearlman, E., Luster, A. D., Leder, P. (1997) Targeted disruption of the chemokine eotaxin partially reduces antigen-induced tissue eosinophilia. *J. Exp. Med.* **185,** 785–790.
32. Hall, G., Houghton, C. G., Rahbek, J. U., Lamb, J. R., Jarman, E. R. (2003) Suppression of allergen reactive Th2 mediated responses and pulmonary eosinophilia by intranasal administration of an immunodominant peptide is linked to IL-10 production. *Vaccine* **21,** 549–561.
33. Tomkinson, A., Duez, C., Cieslewicz, G., Pratt, J. C., Joetham, A., Shanafelt, M. C., Gundel, R., Gelfand, E. W. (2001) A murine IL-4 receptor antagonist that inhibits IL-4- and IL-13-induced responses prevents antigen-induced airway eosinophilia and airway hyperresponsiveness. *J. Immunol.* **166,** 5792–5800.
34. Roy, R. M., Wüthrich, M., Klein, B. S. (2012) Chitin elicits CCL2 from airway epithelial cells and induces CCR2-dependent innate allergic inflammation in the lung. *J. Immunol.* **189,** 2545–2552.
35. Sasisekhar, B., Aparna, M., Augustin, D. J., Kaliraj, P., Kar, S. K., Nutman, T. B., Narayanan, R. B. (2005) Diminished monocyte function in microfilaremic patients with lymphatic filariasis and its relationship to altered lymphoproliferative responses. *Infect. Immun.* **73,** 3385–3393.
36. Semnani, R. T., Keiser, P. B., Coulibaly, Y. I., Keita, F., Diallo, A. A., Traore, D., Diallo, D. A., Doumbo, O. K., Traore, S. F., Kubofcik, J., Klion, A. D., Nutman, T. B. (2006) Filaria-induced monocyte dysfunction and its reversal following treatment. *Infect. Immun.* **74,** 4409–4417.
37. O'Regan, N. L., Steinfelder, S., Venugopal, G., Rao, G. B., Lucius, R., Srikantam, A., Hartmann, S. (2014) *Brugia malayi* microfilariae induce a regulatory monocyte/macrophage phenotype that suppresses innate and adaptive immune responses. *PLoS Negl. Trop. Dis.* **8,** e3206.
38. Egwang, T. G., Kazura, J. W. (1990) The BALB/c mouse as a model for immunological studies of microfilariae-induced pulmonary eosinophilia. *Am. J. Trop. Med. Hyg.* **43,** 61–66.
39. Careau, E., Turmel, V., Lauzon-Joset, J. F., Bissonnette, E. Y. (2010) Alveolar macrophages reduce airway hyperresponsiveness and modulate cytokine levels. *Exp. Lung Res.* **36,** 255–261.
40. Herbert, D. R., Hölscher, C., Mohrs, M., Arendse, B., Schwegmann, A., Radwanska, M., Leeto, M., Kirsch, R., Hall, P., Mossmann, H., Claussen, B., Förster, I., Brombacher, F. (2004) Alternative macrophage activation is essential for survival during schistosomiasis and down modulates T helper 1 responses and immunopathology. *Immunity* **20,** 623–635.
41. Cai, Y., Sugimoto, C., Arainga, M., Alvarez, X., Didier, E. S., Kuroda, M. J. (2014) In vivo characterization of alveolar and interstitial lung macrophages in rhesus macaques: implications for understanding lung disease in humans. *J. Immunol.* **192,** 2821–2829.
42. Cai, Y., Sugimoto, C., Liu, D. X., Midkiff, C. C., Alvarez, X., Lackner, A. A., Kim, W. K., Didier, E. S., Kuroda, M. J. (2015) Increased monocyte turnover is associated with interstitial macrophage accumulation and pulmonary tissue damage in SIV-infected rhesus macaques. *J. Leukoc. Biol.* **97,** 1147–1153.
43. Gillette-Ferguson, I., Hise, A. G., McGarry, H. F., Turner, J., Esposito, A., Sun, Y., Diaconu, E., Taylor, M. J., Pearlman, E. (2004) *Wolbachia*-induced neutrophil activation in a mouse model of ocular onchocerciasis (river blindness). *Infect. Immun.* **72,** 5687–5692.
44. Maus, U. A., Waelsch, K., Kuziel, W. A., Delbeck, T., Mack, M., Blackwell, T. S., Christman, J. W., Schlöndorff, D., Seeger, W., Lohmeyer, J. (2003) Monocytes are potent facilitators of alveolar neutrophil emigration during lung inflammation: role of the CCL2-CCR2 axis. *J. Immunol.* **170,** 3273–3278.
45. Andrews, K., Abdelsamed, H., Yi, A. K., Miller, M. A., Fitzpatrick, E. A. (2013) TLR2 regulates neutrophil recruitment and cytokine production with minor contributions from TLR9 during hypersensitivity pneumonitis. *PLoS One* **8,** e73143.
46. Semnani, R. T., Liu, A. Y., Sabzevari, H., Kubofcik, J., Zhou, J., Gilden, J. K., Nutman, T. B. (2003) *Brugia malayi* microfilariae induce cell death in human dendritic cells, inhibit their ability to make IL-12 and IL-10, and reduce their capacity to activate CD4+ T cells. *J. Immunol.* **171,** 1950–1960.
47. Martín-Gayo, E., Sierra-Filardi, E., Corbí, A. L., Toribio, M. L. (2010) Plasmacytoid dendritic cells resident in human thymus drive natural Treg cell development. *Blood* **115,** 5366–5375.
48. De Heer, H. J., Hammad, H., Soullié, T., Hijdra, D., Vos, N., Willart, M. A., Hoogsteden, H. C., Lambrecht, B. N. (2004) Essential role of lung plasmacytoid dendritic cells in preventing asthmatic reactions to harmless inhaled antigen. *J. Exp. Med.* **200,** 89–98.
49. Maldonado-López, R., De Smedt, T., Michel, P., Godfroid, J., Pajak, B., Heirman, C., Thielemans, K., Leo, O., Urbain, J., Moser, M. (1999) CD8alpha+ and CD8alpha− subclasses of dendritic cells direct the development of distinct T helper cells in vivo. *J. Exp. Med.* **189,** 587–592.
50. Cella, M., Facchetti, F., Lanzavecchia, A., Colonna, M. (2000) Plasmacytoid dendritic cells activated by influenza virus and CD40L drive a potent TH1 polarization. *Nat. Immunol.* **1,** 305–310.
51. Maldonado-López, R., Maliszewski, C., Urbain, J., Moser, M. (2001) Cytokines regulate the capacity of CD8alpha(+) and CD8alpha(−) dendritic cells to prime Th1/Th2 cells in vivo. *J. Immunol.* **167,** 4345–4350.
52. Orr, J. S., Puglisi, M. J., Ellacott, K. L., Lumeng, C. N., Wasserman, D. H., Hasty, A. H. (2012) Toll-like receptor 4 deficiency promotes the alternative activation of adipose tissue macrophages. *Diabetes* **61,** 2718–2727.
53. Turner, J. D., Langley, R. S., Johnston, K. L., Egerton, G., Wanji, S., Taylor, M. J. (2006) *Wolbachia* endosymbiotic bacteria of *Brugia malayi* mediate macrophage tolerance to TLR- and CD40-specific stimuli in a MyD88/TLR2-dependent manner. *J. Immunol.* **177,** 1240–1249.
54. Endo, Y., Nakazawa, N., Liu, Y., Iwaki, D., Takahashi, M., Fujita, T., Nakata, M., Matsushita, M. (2005) Carbohydrate-binding specificities of mouse ficolin A, a splicing variant of ficolin A and ficolin B and their complex formation with MASP-2 and sMAP. *Immunogenetics* **57,** 837–844.
55. Shin, E. H., Osada, Y., Sagara, H., Takatsu, K., Kojima, S. (2001) Involvement of complement and fibronectin in eosinophil-mediated damage to *Nippostrongylus brasiliensis* larvae. *Parasite Immunol.* **23,** 27–37.
56. Shibata, T., Habiel, D. M., Coelho, A. L., Kunkel, S. L., Lukacs, N. W., Hogaboam, C. M. (2014) Axl receptor blockade ameliorates pulmonary pathology resulting from primary viral infection and viral exacerbation of asthma. *J. Immunol.* **192,** 3569–3581.
57. Fujimori, T., Grabiec, A. M., Kaur, M., Bell, T. J., Fujino, N., Cook, P. C., Svedberg, F. R., MacDonald, A. S., Maciewicz, R. A., Singh, D., Hussell, T. (2015) The Axl receptor tyrosine kinase is a discriminator of macrophage function in the inflamed lung. *Mucosal Immunol.* **8,** 1021–1030.
58. Dibbert, B., Daigle, I., Braun, D., Schranz, C., Weber, M., Blaser, K., Zangemeister-Wittke, U., Akbar, A. N., Simon, H. U. (1998) Role for Bcl-xL in delayed eosinophil apoptosis mediated by granulocyte-macrophage colony-stimulating factor and interleukin-5. *Blood* **92,** 778–783.
59. Tai, P. C., Sun, L., Spry, C. J. (1991) Effects of IL-5, granulocyte/macrophage colony-stimulating factor (GM-CSF) and IL-3 on the survival of human blood eosinophils in vitro. *Clin. Exp. Immunol.* **85,** 312–316.
60. O'Byrne, P. M., Inman, M. D., Parameswaran, K. (2001) The trials and tribulations of IL-5, eosinophils, and allergic asthma. *J. Allergy Clin. Immunol.* **108,** 503–508.
61. Zhang, X., Moilanen, E., Kankaanranta, H. (2000) Enhancement of human eosinophil apoptosis by fluticasone propionate, budesonide, and beclomethasone. *Eur. J. Pharmacol.* **406,** 325–332.
62. Ilmarinen, P., Kankaanranta, H. (2014) Eosinophil apoptosis as a therapeutic target in allergic asthma. *Basic Clin. Pharmacol. Toxicol.* **114,** 109–117.

KEY WORDS:
filariasis · flow cytometry · gene expression · alternative activation · proapoptotic genes